Transactions of the SMiRT 27
Yokohama, Japan, March 3-8, 2024
Division V

APPLICABILITY OF LARGE-SCALE SEISMIC RESPONSE ANALYSIS TO NUCLEAR POWER BUILDING BASED ON FINITE ELEMENT MODELING

Eiji Tanaka[1], Takaaki Tsukada[1], Yasuhiro Ohashi[1]

[1] Shimizu Corporation, Tokyo, Japan (tanaka_e@shimz.co.jp)

ABSTRACT

This paper presents a large-scale nonlinear analysis of a turbine building of a nuclear power plant. The turbine building consists of a turbine pedestal and building frame covering it, which deform independently when an earthquake occurs. The pedestal and frame have a gap; however, a concern is that future megathrust earthquakes could cause their collisions, which can be critical for evaluating the seismic response. Considering these complex phenomena, numerical modeling and analysis should be conducted for the seismic safety assessment of nuclear power buildings.

In this study, a fully three-dimensional finite element model of a turbine building using solid elements was examined to precisely compute the stress distribution and deformation caused by a collision. However, a fully solid element model is computationally expensive; therefore, a large-scale parallel analysis was conducted to improve the efficiency. Furthermore, we introduced a contact analysis procedure based on the penalty method into the large-scale analysis to address the boundary nonlinearity characterizing the collision behavior. The proposed analysis method was validated by comparing the experimental results of a drop weight test and numerical results.

The reinforced concrete structure of the turbine building was discretized using solid elements, and the numerical results showed that the fully solid element model provided a more detailed and adequate solution than a conventional lumped mass model. Therefore, the proposed analysis method can be applied to large-scale nonlinear problems of nuclear power buildings.

INTRODUCTION

Currently, obtaining detailed information about structural damage, such as the distribution of local failure and response acceleration, is crucial for the seismic safety assessment of nuclear power plants. In Japan, conventional structural calculations for the seismic design of nuclear power buildings have been performed using a lumped mass model (LMM) based on beam and spring elements, whereas three-dimensional finite element models (3D FEMs) have been employed in other countries [ASCE (2017)]. An LMM has advantages in terms of computational speed and cost; however, it is not necessarily required owing to the recent development of computers that enable the computing of complex analyses, such as 3D FEMs. Thus, several studies [Onitsuka et al. (2019)] [Choi et al. (2022)] have applied 3D FEMs using solid elements to the seismic analysis of nuclear power buildings and showed that they can appropriately account for the 3D dynamic behavior, material nonlinearity, and soil–structure interaction of such buildings.

On the contrary, it is necessary to consider the extreme loading situations caused by collisions, such as accidental aircraft crashes, for the safety assessment. Some experimental studies have been conducted on components of buildings [Hashimoto et al. (2005)]; however, estimating how a local crash affects an entire building based solely on these results is difficult. Furthermore, a concern is that future megathrust earthquakes could cause collisions of building structures, which can be critical for their seismic safety assessment. For example, a turbine building consists of a turbine pedestal and building frame covering it, which deform independently and can collide when an earthquake occurs, as shown in Figure 1. Therefore, an entire building must be simulated using an elaborate 3D FEM to assess the risk of crashes and improve plant safety.

In this study, a nonlinear dynamic analysis of a nuclear power building crash was conducted using a fully solid finite element model. A fully solid element model is computationally expensive; therefore, a large-scale parallel analysis procedure based on open-source code FrontISTR [Ito and Okuda (2006)] was employed to improve efficiency. Furthermore, we introduced a contact analysis procedure and the material constitutive law of reinforced concrete (RC) into the large-scale analysis to address the collision behavior. The applicability of the proposed analysis method was demonstrated by two numerical examples. First, a numerical analysis of a drop weight test was conducted to demonstrate the validity and accuracy of the analysis method. Second, the collision analysis of a turbine building was conducted, and the numerical results were compared with those of an LMM.

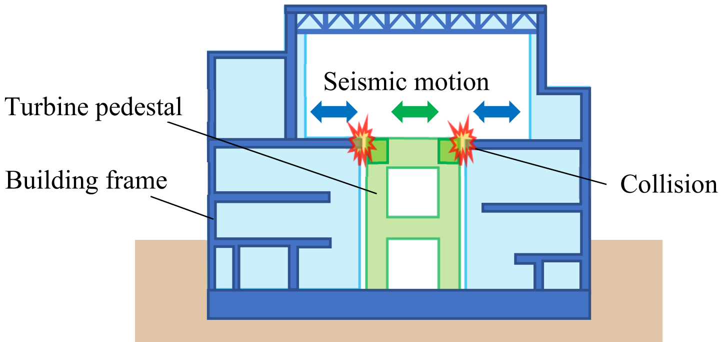

Figure 1. Schematic of collision in turbine building

VALIDATION OF ANALYSIS METHOD USING DROP WEIGHT TEST

Test Specimen and Analysis Model

The analysis method was validated by comparing the numerical results of this study with experimental results reported in the literature [Tanoue et al. (2013)]. Specifically, a weight was dropped on an RC specimen, postulating an aircraft impact. The test specimen was an RC box frame (Figure 2), which was 3 m wide, 1 m high, and 1 m deep. The compressive strength of the concrete was 33 N/mm^2 and the yield strength of the rebar was 345 N/mm^2. Pinned supports were placed at the bottom of the specimen and additional weight plates were placed on the upper and lower floors of the specimen to ensure consistency with the eigenfrequency of the actual floor of the reactor building. A weight of 300 kg was dropped from 10 m above the top center of the upper floor of the specimen, on which a rubber buffer was set to adjust the load duration to that of the actual aircraft impact.

The analysis model is shown in Figure 3. A quarter of the specimen and experimental equipment were modeled because of symmetry, and the mesh consisted of eight-node hexahedral elements. A central additional weight was modelled using solid elements and other weights were modelled as nodal masses. A nut above a top plate was semi-rigidly connected to a bottom plate. To simulate cracks in concrete, a nonorthogonal multidirectional smeared crack model [Maekawa et al. (2003)] was employed as the material constitutive law. When a crack occurs, this model defines the local coordinate system of the crack plane and employs anisotropic stress–strain relationships, as shown in Figure 4. Local stress was obtained by considering the softening caused by cracks, and we employed a bilinear softening model as the tensile stress–strain relationship and a modified Ahmad model as the compressive stress–strain relationship in this study. In addition, solid elements of the specimen considering both concrete and rebar embedded in the concrete are expressed as follows:

$$\boldsymbol{\sigma} = \mathbf{r}_S{}^T \boldsymbol{\sigma}_S + \boldsymbol{\sigma}_C \tag{1}$$

where $\boldsymbol{\sigma}$ is the stress of the specimen, $\mathbf{r}_S$ is the spatial occupancy rate of the embedded rebar, $\boldsymbol{\sigma}_S$ is the stress of the embedded rebar, and $\boldsymbol{\sigma}_C$ is the stress of the concrete. Furthermore, $\boldsymbol{\sigma}_S$ was derived using a modified Menegotto–Pinto model [Menegotto and Pinto (1973)] to consider the material plasticity of the rebar. The rubber buffer was a hyperelastic material and underwent large deformations during the collision of the drop weight. Therefore, we employed the Arruda–Boyce model and considered geometrical nonlinearity. Furthermore, the contact, slip, and separation between the top plate and other objects (e.g., drop weight) were treated using the penalty method to solve the collision problem. The contact, slip, and separation between the rubber buffer and other objects were also treated using the penalty method.

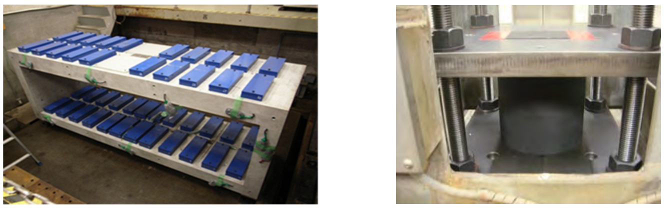

(a) Test specimen (b) Rubber buffer

Figure 2. Drop weight test [Tanoue et al. (2013)]

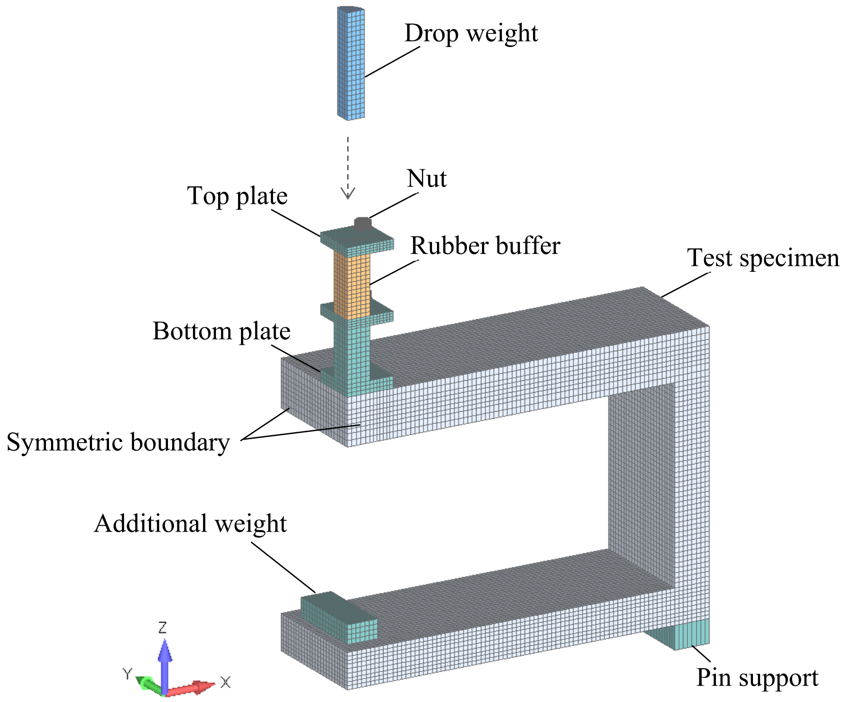

Figure 3. Analysis model of drop weight test

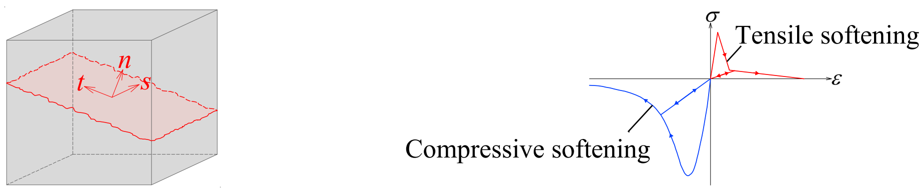

(a) Local coordinate system of crack plane (b) Local stress–strain relationship

Figure 4. Schematic of smeared crack model

Numerical Results

Table 1 summarizes the numerical results of the eigenvalue analysis and the experimental results of a hammering test reported in the literature [Tanoue et al. (2013)] where we omit the asymmetric first eigenmode. The eigenfrequencies and mode shapes from the numerical results are similar to those from the experimental results, and the analysis model simulates the vibration characteristics obtained from the experiment.

Figure 5 depicts the crack distribution of the concrete and the deformation obtained by the dynamic analysis based on a direct time integration method, where the red lines of the opening crack plane are plotted on the deformed representation. After the collision of the drop weight, a crack initiates at approximately 0.526 s, which is the time to reach the maximum contact force. The crack extends until approximately 0.542 s, which is the time to reach the maximum downward displacement of the upper floor. Subsequently, the upper floor and rubber buffer deform upward, and the nut collides with the top plate at approximately 0.583 s. Finally, the drop weight bounces. These numerical results agree with the motion of the drop weight and crack distribution observed in the experiment.

Table 1. Eigenvalue analysis results of drop weight test specimen

Mode		Analysis	Experiment
2	Eigenfrequency	34.7 Hz	37.3 Hz
	Mode shape	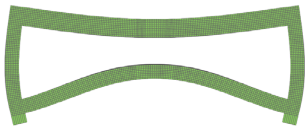	
3	Eigenfrequency	47.6 Hz	48.9 Hz
	Mode shape	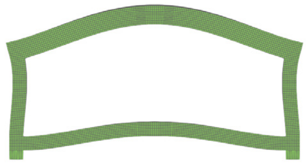	

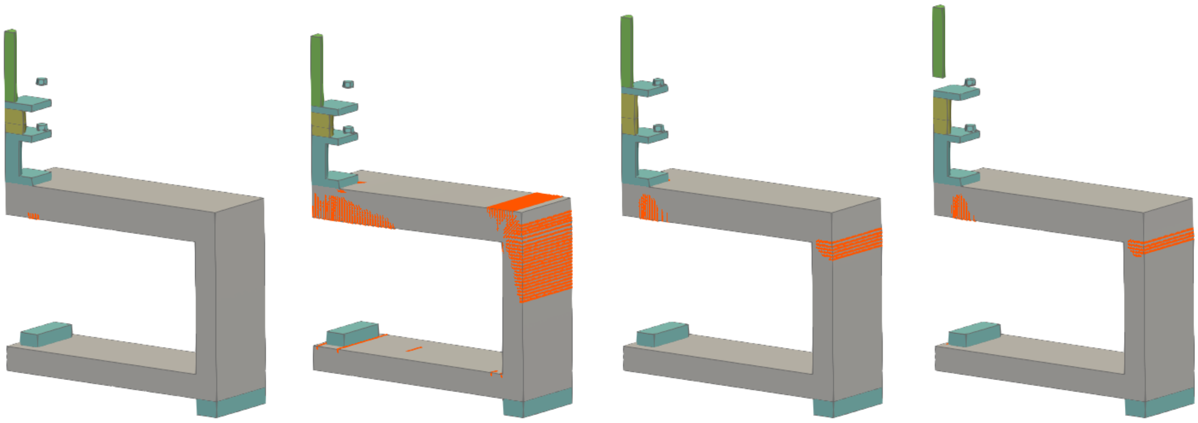

(a) 0.526 s (b) 0.542 s (c) 0.583 s (b) 0.6 s

Figure 5. Crack distribution and deformation of drop weight test

Figure 6 shows the time history of the vertical contact force. The numerical results are in good agreement with the experimental results, indicating that we can adequately solve the dynamic collision problem using the proposed analysis method. Figure 7 shows the time histories of the vertical

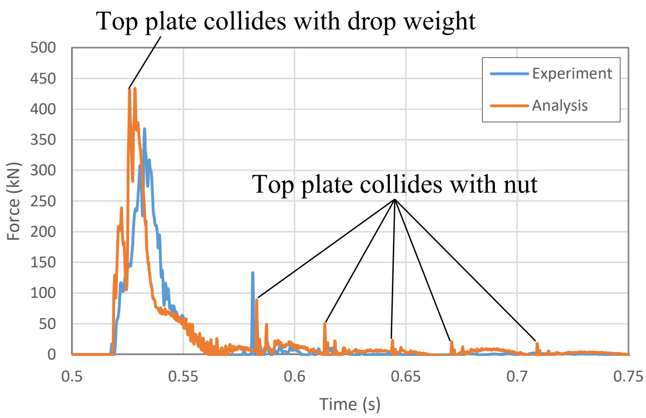

Figure 6. Time history of vertical contact force

accelerations of the upper and lower floors of the specimens. The accelerations of the numerical results agree well with the experimental results, except for the pulse waves of the upper floor at approximately 0.532, 0.583, 0.615, 0.644, 0.671, and 0.709 s. These differences appear to be due to the assumption of symmetry in the analysis model. Pulse waves were observed when the top plate collided with the drop weight and nut; however, the experiment was not completely symmetric, which probably misaligned the position and timing of the collision. Therefore, the validity of the proposed analysis method is demonstrated.

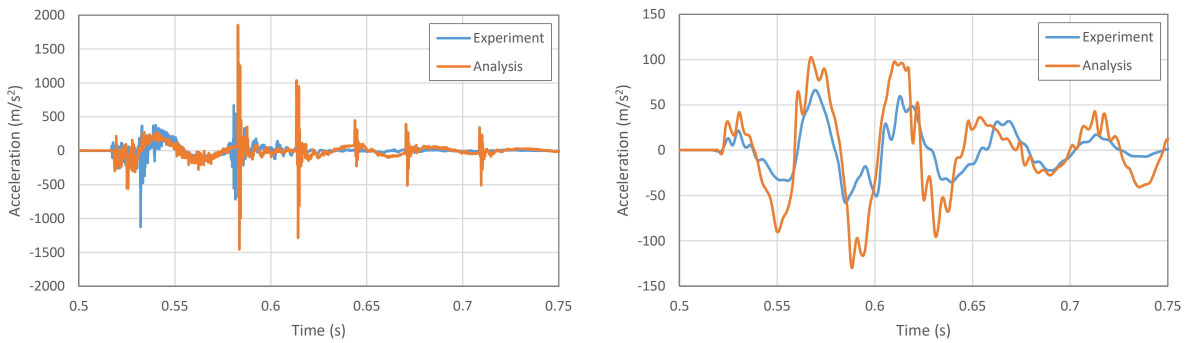

(a) Center of upper floor (b) Center of lower floor

Figure 7. Time histories of vertical accelerations

LARGE-SCALE SEISMIC ANALYSIS OF TURBINE BUILDING

Analysis Models

Following the validation, we conducted a seismic analysis of a turbine building whose specifications were assumed for this study. Figure 8 shows the analysis models, where the turbine building is 101 m long, 82 m wide, and 50 m high. The turbine pedestal and building frame covering it have a gap of 25 mm. A seismic wave is imposed in the y-direction, which causes a collision between the pedestal and frame, as shown in Figure 9. The building consists of a linear elastic material with a Young's modulus of 30,000 N/mm^2, a Poisson's ratio of 0.2, and a density of 2396 kg/m^3.

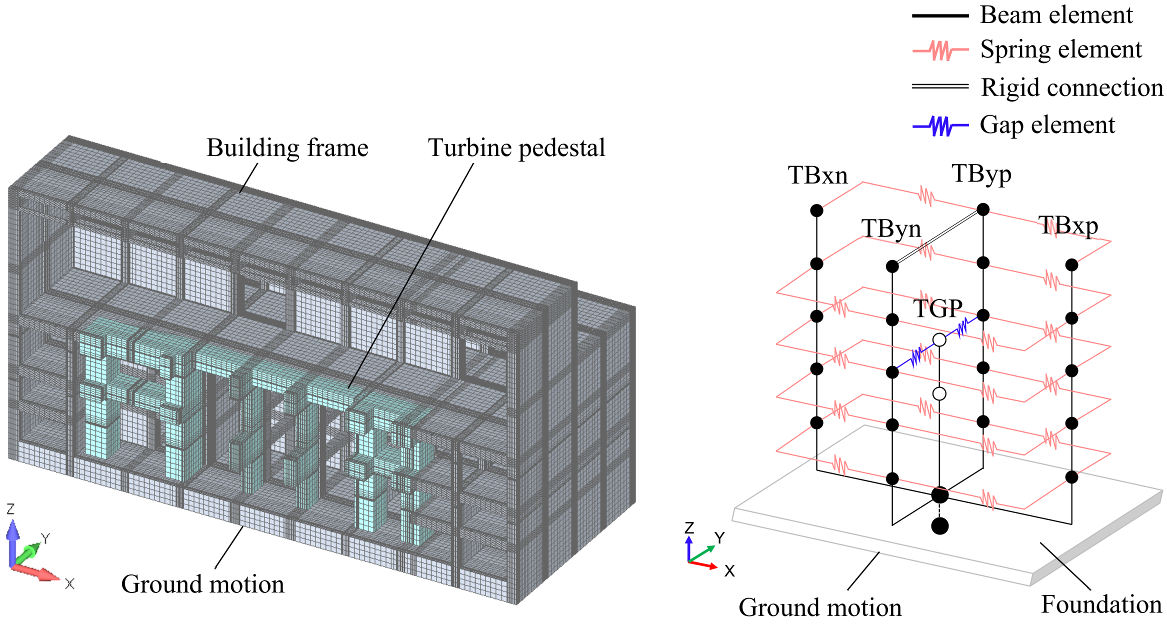

(a) 3D FEM (b) LMM

Figure 8. Analysis models of turbine building

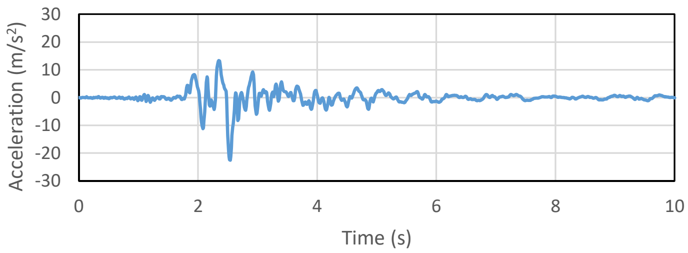

Figure 9. Y-acceleration time history of input seismic wave

We used a 3D FEM and an LMM to compare the discretization methods. The 3D FEM consisted of hexahedral elements except for a few prism elements, and the penalty method was employed to address the collision problem. The number of nodes was 2,105,415 and the number of elements was 1,840,526. We used a matrix solver based on the conjugate gradient method with algebraic multigrid preconditioning and flat-MPI parallel computing based on the domain decomposition method. The LMM consisted of lumped mass nodes, beam elements, and spring elements. The LMM nodes of each floor represented the four sections (TByn, TByp, TBxn, and TBxp) of the frame and pedestal (TGP), and the LMM elements represented the structures between them, such as walls, columns, beams, and slabs. In addition, gap elements were set between the top node of the pedestal and the node of the frame on the same floor to consider collisions.

Table 2 presents the numerical results of the eigenvalue analysis. The eigenfrequencies of the 3D FEM agree well the LMM results, indicating that the vibration characteristics of the two models have a similar trend.

Table 2. Eigenvalue analysis results of turbine building

Mode		Eigenfrequency (Hz)	
		3D FEM	LMM
Turbine pedestal	1	5.51	5.62
Building frame	1	5.66	6.12
	2	12.07	11.35

Numerical Results of Seismic Analysis

In addition to a nonlinear seismic analysis considering collisions, we also conducted a linear analysis ignoring collisions, for comparison. Figure 10 and 11 show the distributions of the maximum floor acceleration and displacements, where the floor responses of the 3D FEM are based on the nodes whose positions correspond to the LMM nodes as shown in Figure 12. In addition, the floor responses of TGP are obtained with the average responses of four nodes around the center of the pedestal, as shown in Figure 12. Figure 10, which presents the case ignoring collisions, shows that the responses of the 3D FEM agree well to those of the LMM, except for TBxn and TBxp. The responses of TByn, TByp, TBxn, and TBxp of the LMM are similar; therefore, the LMM spring elements connecting the nodes on the same floor are overestimating the in-plane stiffness of each floor. Moreover, the LMM deforms like a rigid floor compared to the 3D FEM. Figure 11, which presents the case considering collisions, shows that the accelerations of TByn, TByp, and TGP of the LMM increase remarkably when the floors collide with each other. In contrast to the LMM results, the responses of the 3D FEM considering collisions are similar to those when collisions are ignored.

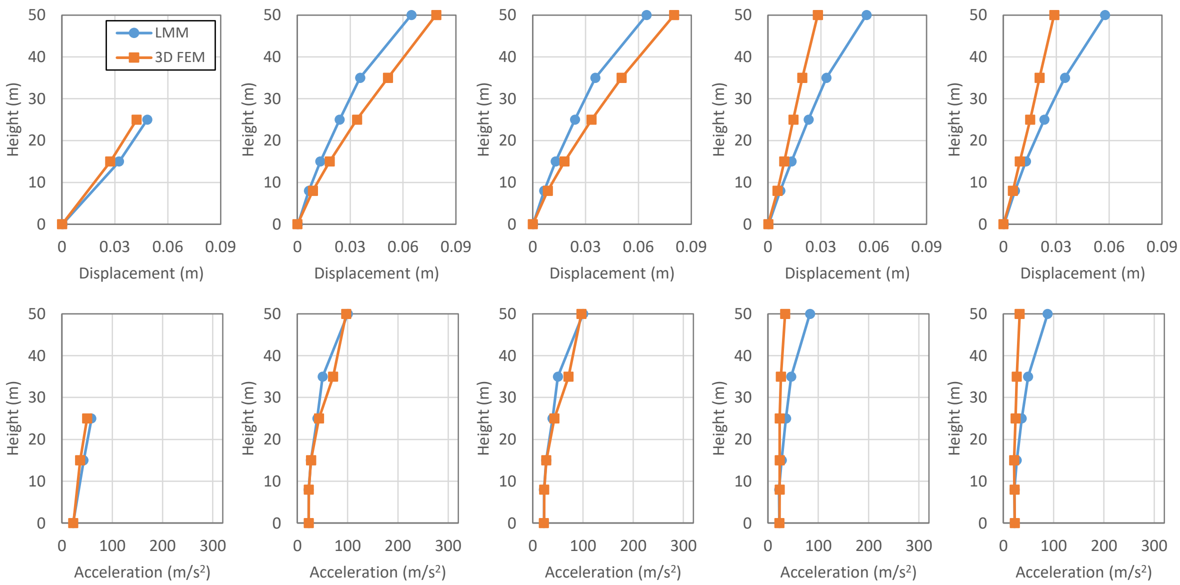

(a) TGP (b) TByn (c) TByp (d) TBxn (e) TBxp

Figure 10. Maximum responses in y-direction of turbine building ignoring collisions

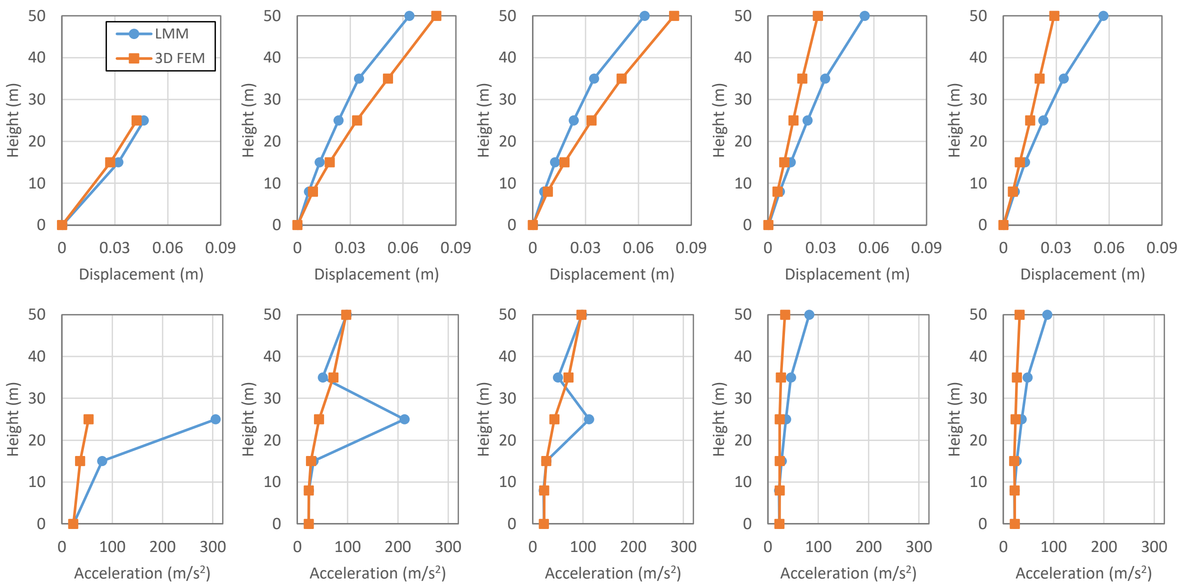

(a) TGP (b) TByn (c) TByp (d) TBxn (e) TBxp

Figure 11. Maximum floor responses in y-direction of turbine building considering collisions

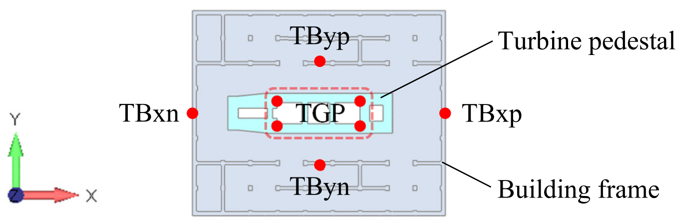

Figure 12. Nodes of 3D FEM to compare with floor responses of LMM

By contrast, the maximum acceleration distribution of the 3D FEM depends on the collision, as shown in Figure 13. In the 3D FEM, the edge of the pedestal collides with the TByn side edge of the frame, and the acceleration near the collision point increases more locally than that in the LMM. In

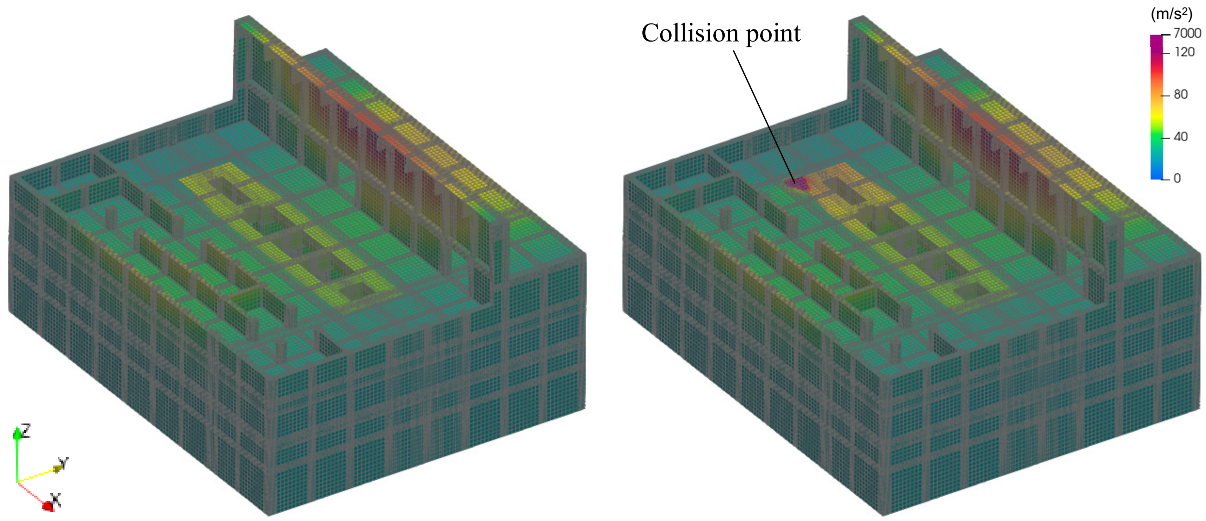

(a) Ignoring collision (b) Considering collision

Figure 13. Maximum acceleration distribution in y-direction of 3D FEM

addition, maximum acceleration near the collision point is greater than 300 m/s^2, which is the maximum TGP floor acceleration of the LMM. The collision does not affect the acceleration distribution of the 3D FEM, except near the collision point. However, it affects the floor acceleration of the LMM over a wide area represented by a lumped mass node. Therefore, the 3D FEM can capture local collision behavior better than the LMM.

Figure 14 shows the time histories of the floor acceleration and displacement of TGP, and Figure 15 shows those of the acceleration and displacement of the 3D FEM node near the collision point. The floor responses of the LMM agree with those of the 3D FEM before the first collision and when the collision is ignored. However, TGP of the LMM collides with TByp and TByn after the first collision between TGP and TByn, whereas TGP of the 3D FEM collides with TByn only once. Thus,

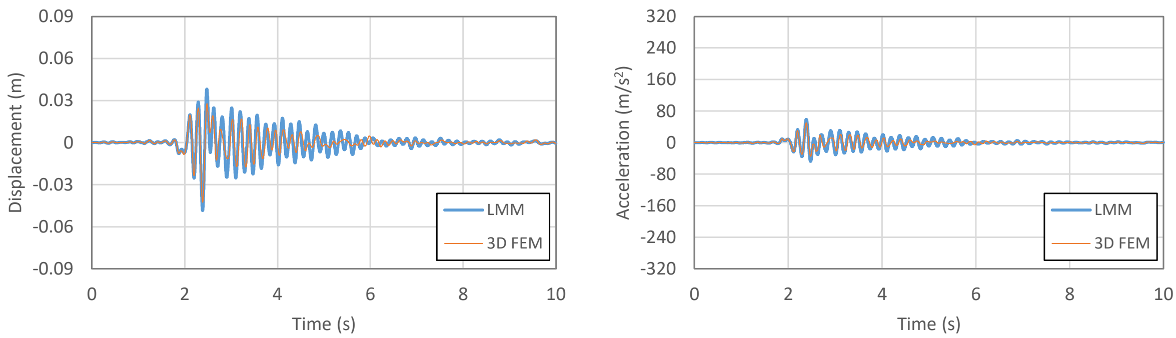

(a) Ignoring collision

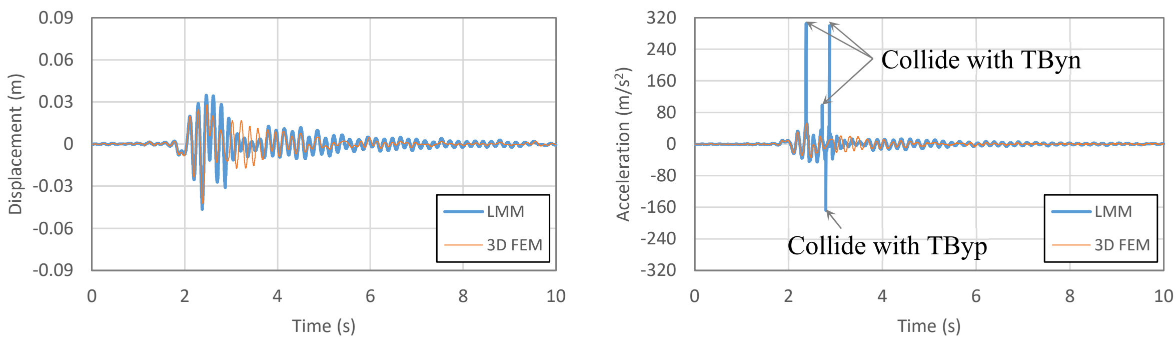

(b) Considering collision

Figure 14. Floor response time histories of TGP top node

expressing the local behavior of a collision using a 3D FEM is important for simulating the motion after the collision.

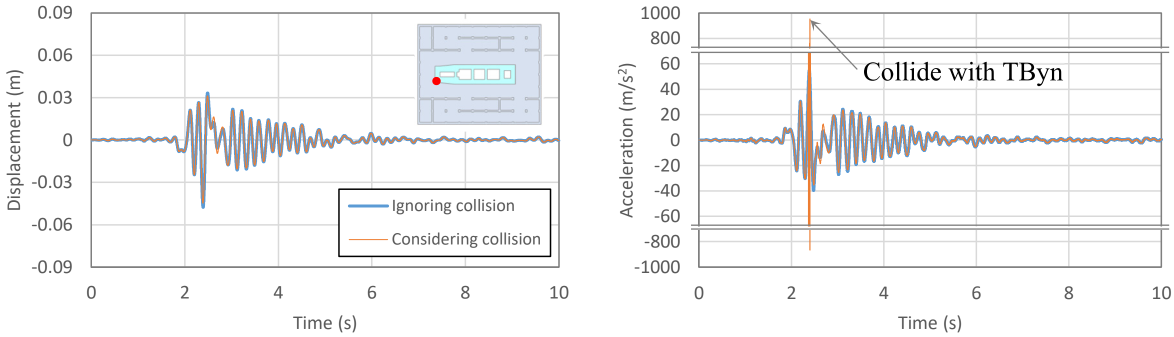

Figure 15. Response time histories near collision point of 3D FEM

CONCLUSION

In this study, large-scale nonlinear analysis of a nuclear power building was conducted. The building was discretized as a fully 3D finite solid element model, and a large-scale parallel analysis procedure was employed to improve the computational efficiency. First, the proposed analysis method was validated by comparing the experimental results of a drop weight test with the numerical results. We showed that the proposed analysis method could estimate the nonlinear dynamic behavior of a collision. Second, a large-scale nonlinear analysis of a nuclear turbine building was conducted, and the numerical results indicated that the 3D finite solid element model could appropriately deal with the local behavior of a collision compared to a conventional LMM. Therefore, the proposed analysis method can be applicable to the safety assessment of seismic and extreme loading situations, such as collisions, through future studies considering material nonlinearities and comparison of numerical results and real phenomena.

REFERENCES

American Society of Civil Engineers. (2017). "Seismic analysis of safety-related nuclear structures", ASCE, Reston, Virginia, USA.

Onitsuka, S., Iijima, T., Yamada T., Yoshimura, S. (2019). "Seismic analysis of nuclear power plants by using three-dimensional finite element models: a review", Journal of Nuclear Science and Technology, Vol. 56, 1, 1-16.

Choi, B., Nishida, A., Kawata, M., Shiomi T., Li, Y. (2022). "Standard Guideline for the Seismic Response Analysis Method Using 3D Finite Element Model of Reactor Buildings", JAEA-Research, JAEA, Ibaraki, Japan, 2021-017.

Hashimoto, J., Takiguchi, K., Nishimura, K., Matsuzawa, K., Tsutsui, M., Ohashi., Y., Kojima, I., Torita, H. (2005). "Experimental Study on Behavior of RC Panels Covered with Steel Plates Subjected to Missile Impact", SMiRT 18, J05-4.

Ito, S. and Okuda, H. (2006). HPC-MW: "A problem solving environment for developing parallel FEM application", Applied Parallel Computing, State of the Art in Scientific Computing, LNCS4699, 694-702.

Tanoue, T., Ikeda, R., Kawamoto, Y., Beppu, M. (2013). "Experimental Study on Vibration of Concrete Structure with regard to Dropping Impact", SMiRT 22, Division IX.

Maekawa, K., Pimanmas, A., Okamura, H. (2003). "Nonlinear Mechanics of Reinforced Concrete", CRC Press, Boca Raton, Florida, USA.

Menegotto, M., Pinto, P. E. (1973). "Method of Analysis for Cyclically Loaded R. C. Plane Frames Including Changes in Geometry and Non-Elastic Behavior of Elements under Combined Normal Force and Bending", Proc. of IABSE Symposium on Resistance and Ultimate Deformability of Structures Acted on by Well Defined Repeated Loads, 15-22